



Joint Weather & Climate Research Programme – a partnership in weather and climate research

Observing Earth's Energy Imbalance



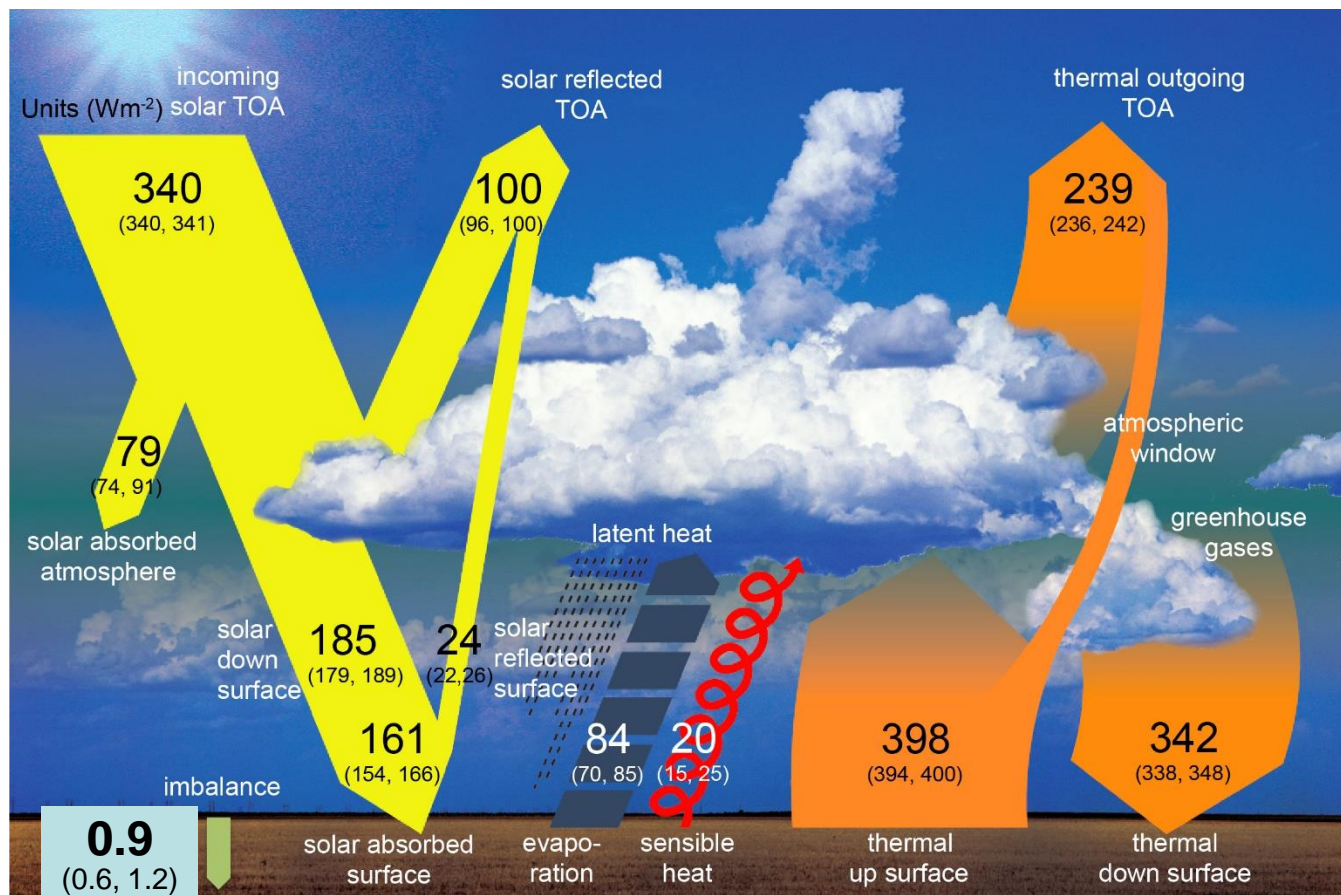
Till Kuhlbrodt, NCAS,
University of Reading,
UK

2nd April 2019



- ① Earth's energy imbalance: definition and implications
- ① Observing Earth's energy imbalance
 - Remote sensing of the radiation balance at the top of the atmosphere
 - In-situ observations of ocean heat content
 - Remote sensing of thermosteric sea level rise
- ① Outlook: what we need to do
- ① Using materials from Benoit Meyssignac, Richard Allan, Karina von Schuckmann and others

Global mean energy budget



IPCC AR5 WGI ch.2

- ⦿ $(0.6 \pm 0.4) \text{ W m}^{-2}$ imbalance diagnosed from ocean data, 2005 to 2010 (Loeb et al. 2012)
- ⦿ More recent estimate: $(0.9 \pm 0.3) \text{ W m}^{-2}$, for 2005 to 2014 data (Trenberth and Fasullo 2016)
- ⦿ Geothermal heat flux is about 0.1 W m^{-2}

Radiation balance

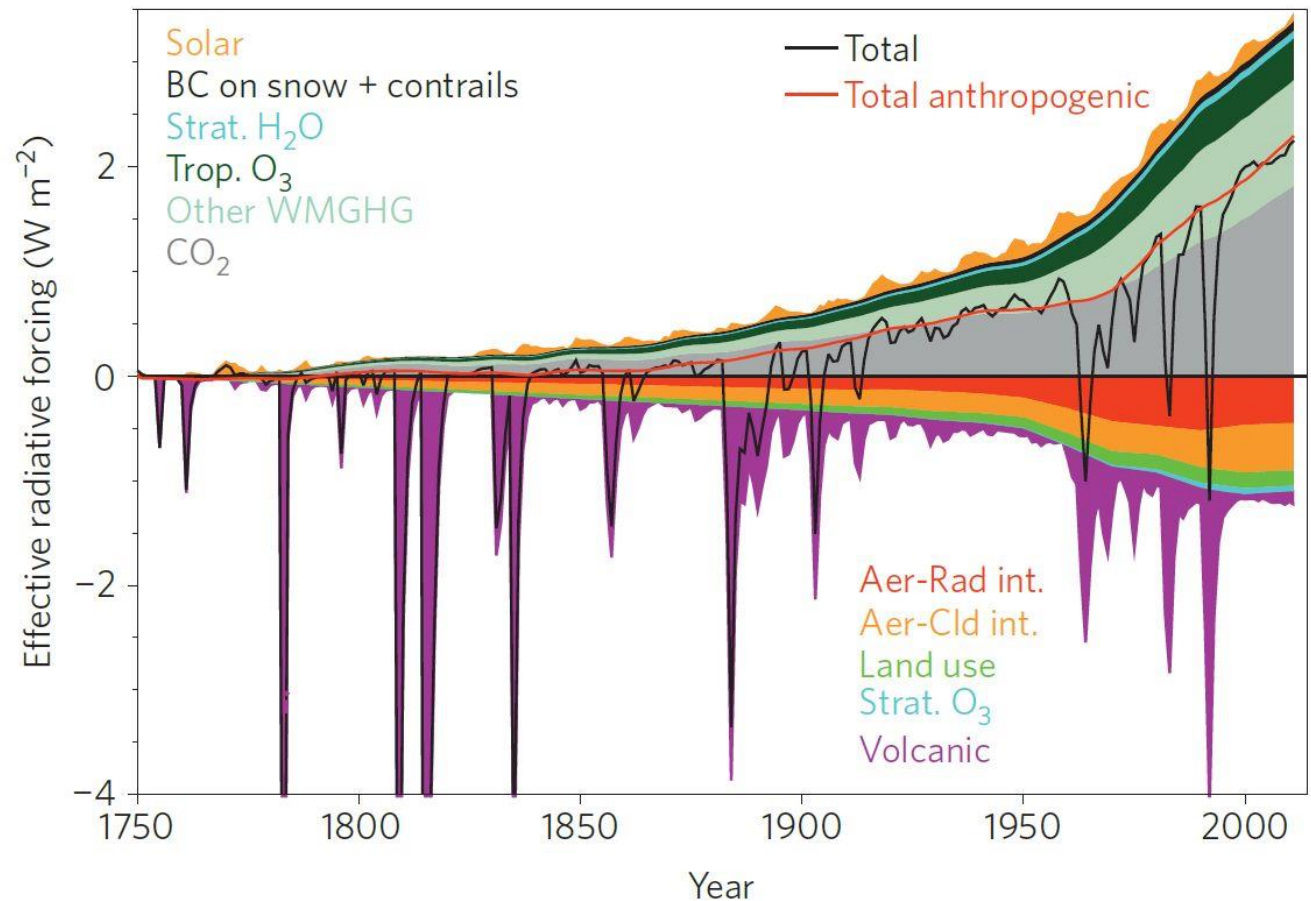


- ⦿ In the absence of perturbations, the net TOA radiation budget would be zero = no energy imbalance.
- ⦿ Earth system is permanently perturbed by external forcing or internal variability, hence always adjusting in response to these
- ⦿ Steady state actually never reached

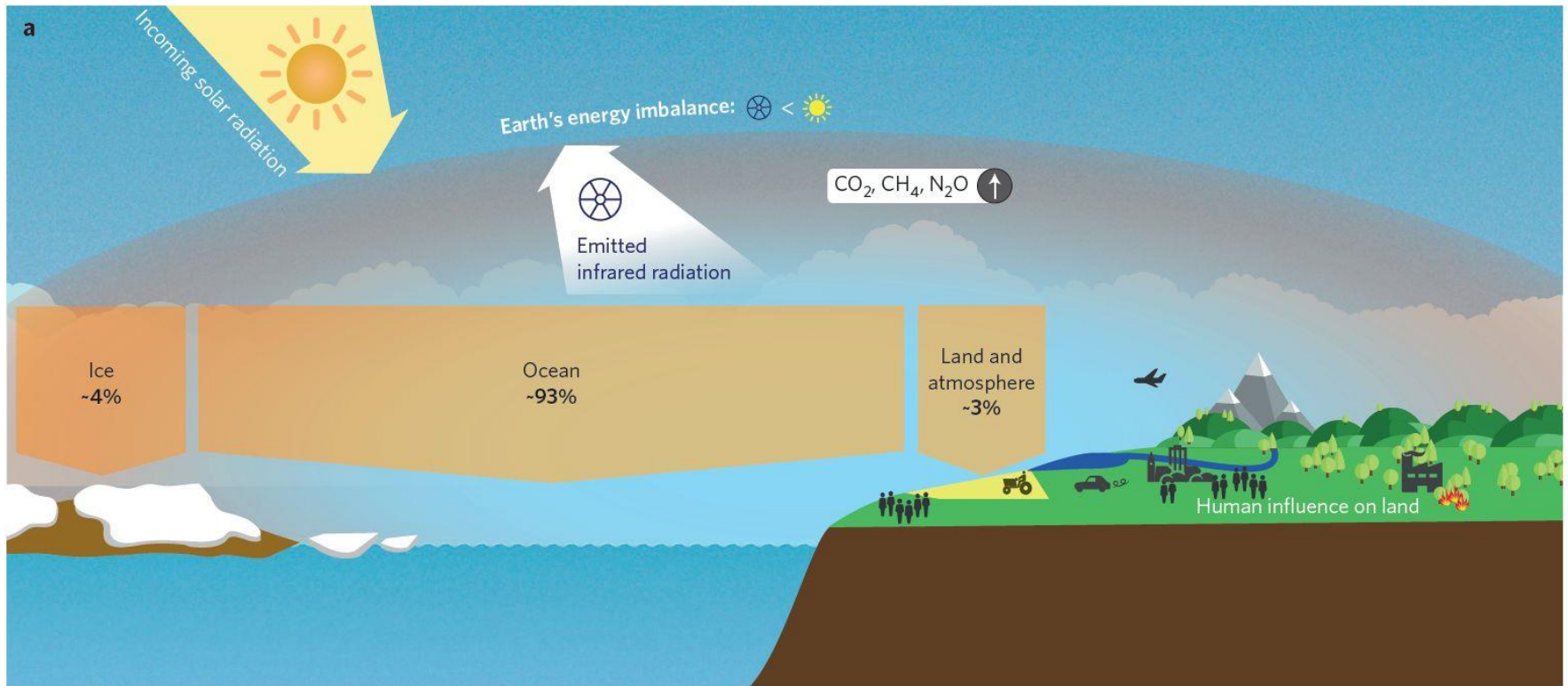
Effective radiative forcing since 1750

Anthropogenic radiative forcing:

- Greenhouse gases
- Aerosols (non-volcanic)
- Land-use change
- Black carbon
- Ozone (stratospheric and tropospheric)
- Stratospheric water vapour

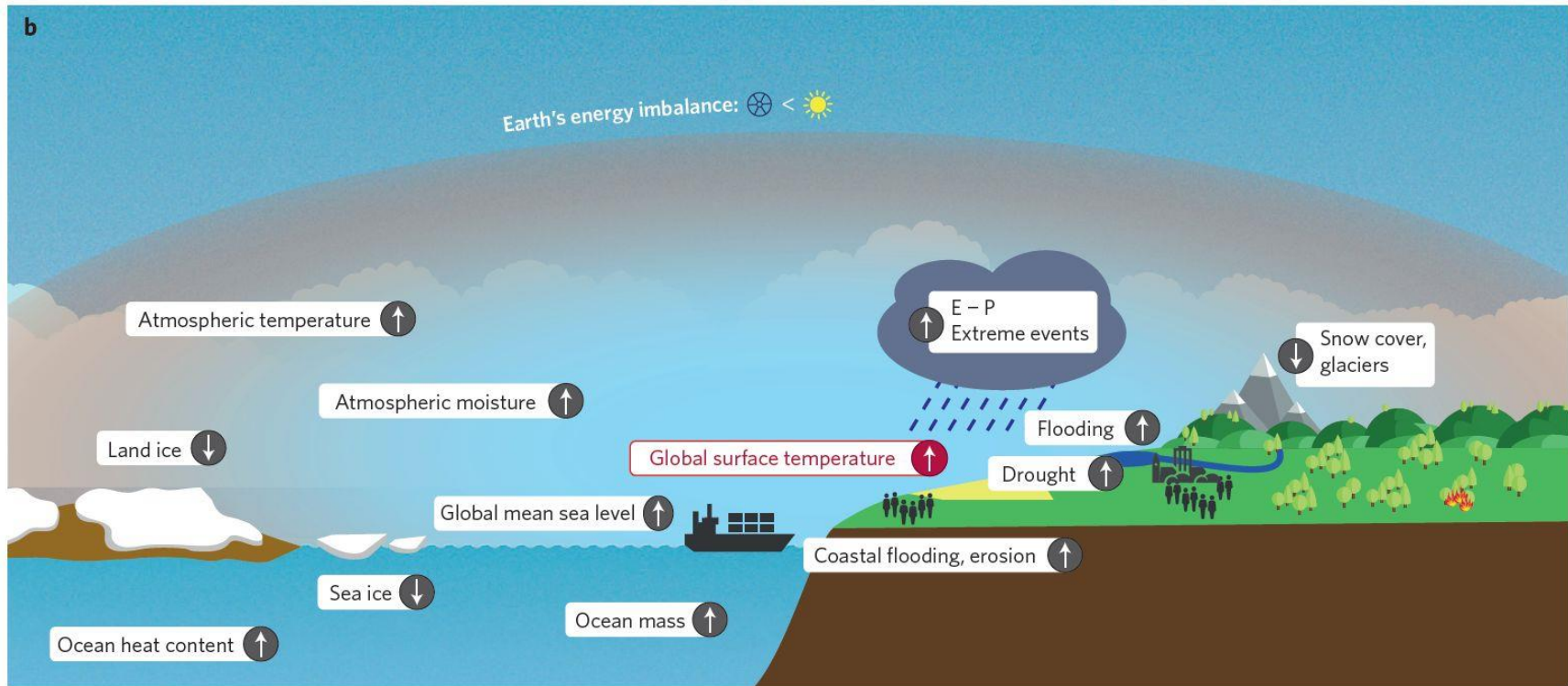


Earth's energy imbalance (EEI)



- EEI results from the integrated response of the climate system to past and present internal and external perturbations
- Time scales from days to 10^4 years – hence EEI variability on these time scales
 - Up to interannual: Internal modes: MJO, ENSO, NAO
 - Decadal and longer: solar radiation, large volcanoes, GHGs

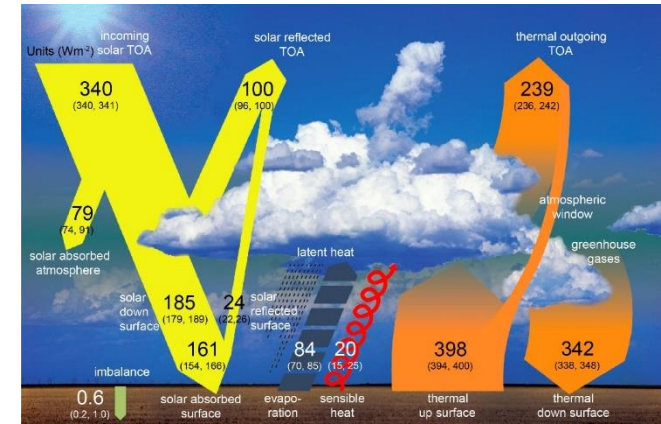
Earth's energy imbalance (EEI): implications



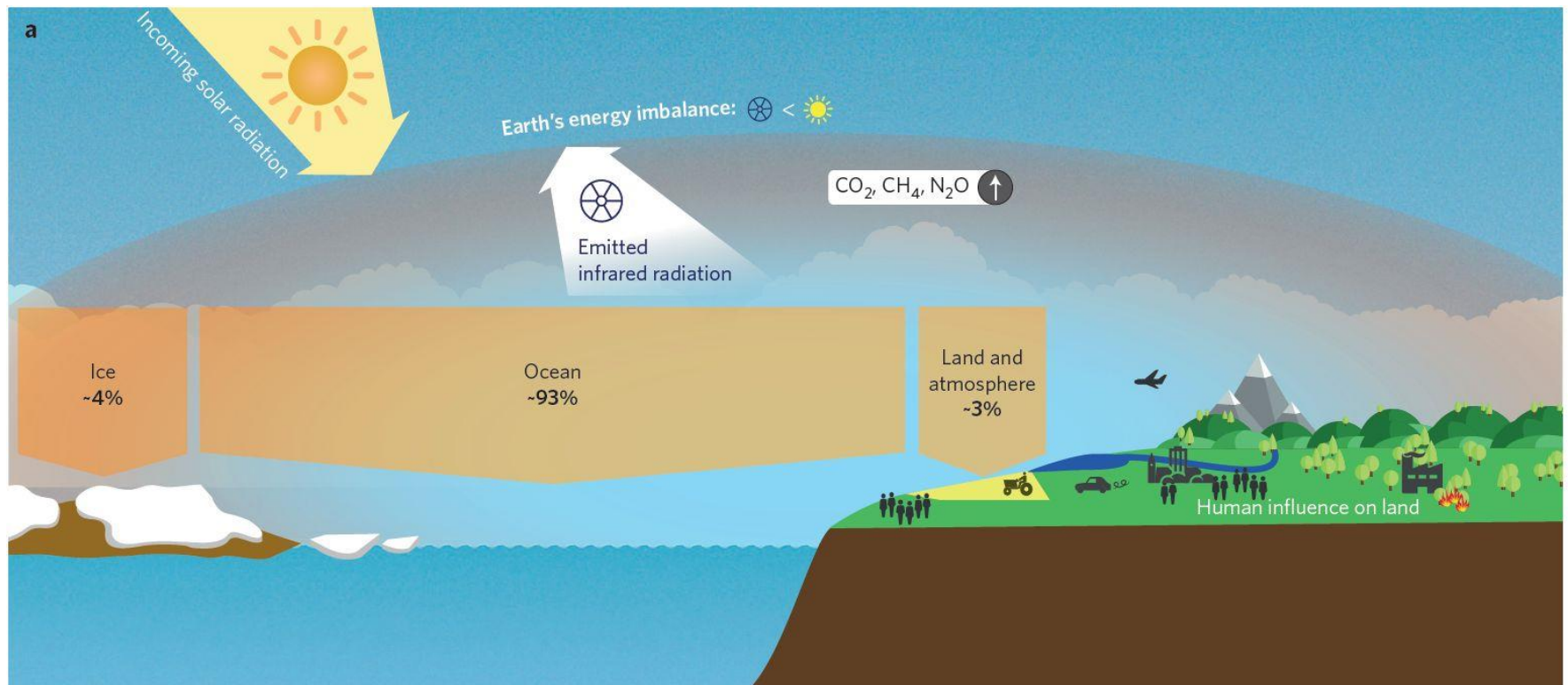
- ⦿ Anthropogenic emissions are the dominant cause of EEI over the last decades
- ⦿ **Integrating EEI over time** gives an estimate of the additional energy stored in the Earth system

Measuring EEI: challenges

- EEI is the residual of large fluxes
- Response to GHG forcing (decades to centuries, $<1 \text{ W m}^{-2}$) buried in noise from monthly to interannual time scales ($\sim 1 \text{ W m}^{-2}$)
- Measurement accuracy of $<0.3 \text{ W m}^{-2}$ (decadal time scale) needed to evaluate **long-term mean EEI** from anthropogenic forcing
- For monitoring GHG mitigation policies in the future on time scales < 10 years, accuracy of $< 0.1 \text{ W m}^{-2}$ is required



Measuring the EEI



- ⦿ At TOA
- ⦿ Surface energy budget
- ⦿ Indirectly: models
- ⦿ Indirectly: inventory

Four ways to estimate the EEI



- 1) Remote sensing of net radiation balance at the top of the atmosphere (TOA)
 - Pro: measure exactly the quantity we're interested in. Satellite data available (CERES) in high temporal resolution
 - Con: Satellite data not good at giving absolute global mean values: $\pm 4 \text{ W m}^{-2}$ (instrument calibration)

Four ways to estimate the EEI



- 1) Remote sensing of net radiation balance at TOA
- 2) Surface energy budget (land and ocean)
 - Estimates from either observations or reanalyses
 - Uncertainty is currently $\pm 15 \text{ W m}^{-2}$

Four ways to estimate the EEI



- 1) Remote sensing of net radiation balance at TOA
- 2) Surface energy budget
- 3) **Climate models**
 - Take various radiative forcings and responses into account
 - Models often have biases. Variation across models is $\pm 0.21 \text{ W m}^{-2}$ at decadal time scales from model spread

Four ways to estimate the EEI



- 1) Remote sensing of net radiation balance at TOA
- 2) Surface fluxes
- 3) Climate/ Earth system models
- 4) Inventory of the energy stored in the Earth system
 - Cover atmosphere, land, cryosphere, ocean
 - Best accuracy so far: $+0.7 \pm 0.7 \text{ W m}^{-2}$ (across different estimates)
 - Used to “anchor” the CERES observations
 - Different energy forms: internal energy, latent heat, potential energy, kinetic energy
 - Internal energy and latent heat dominate at large scale (Trenberth et al., 2002)

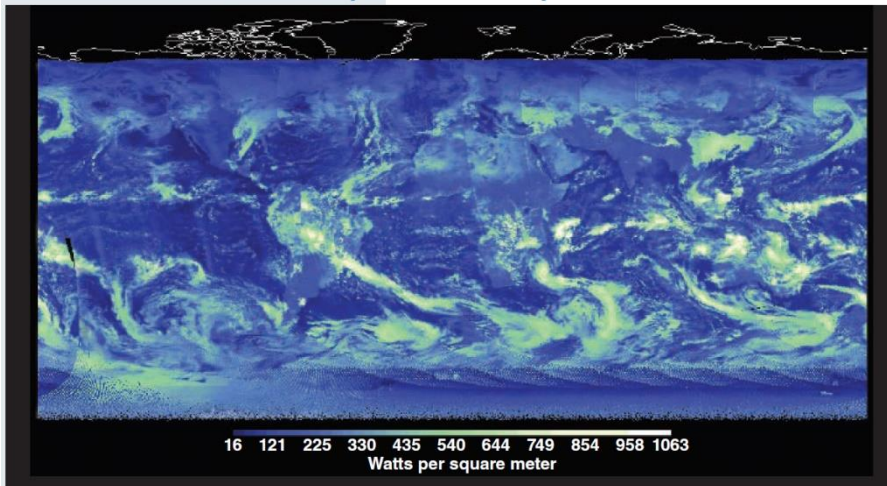
CERES satellite-borne observations

- ☉ **C**louds and the **E**arth's **R**adiant **E**nergy **S**ystem
- ☉ Three channels for measuring radiances: SW, LW, total
- ☉ Currently 6 CERES FM6 instruments in space

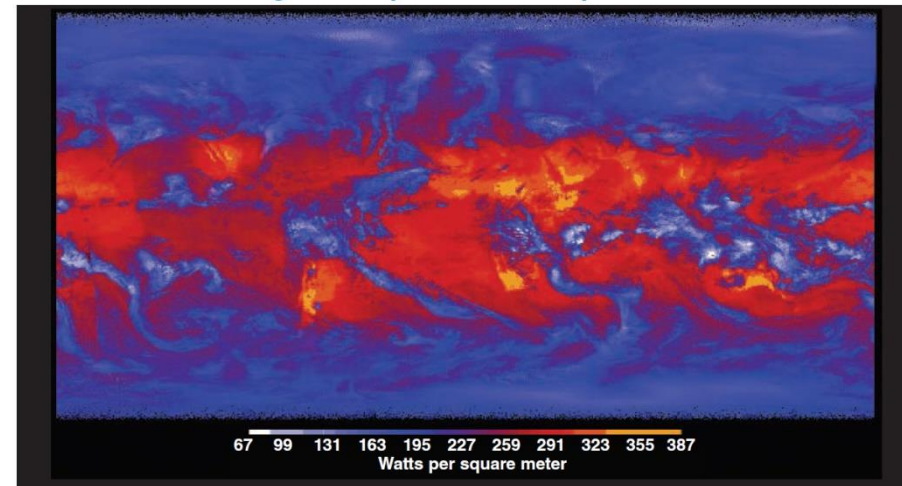


JPSS-1

Shortwave Top of the Atmosphere Flux

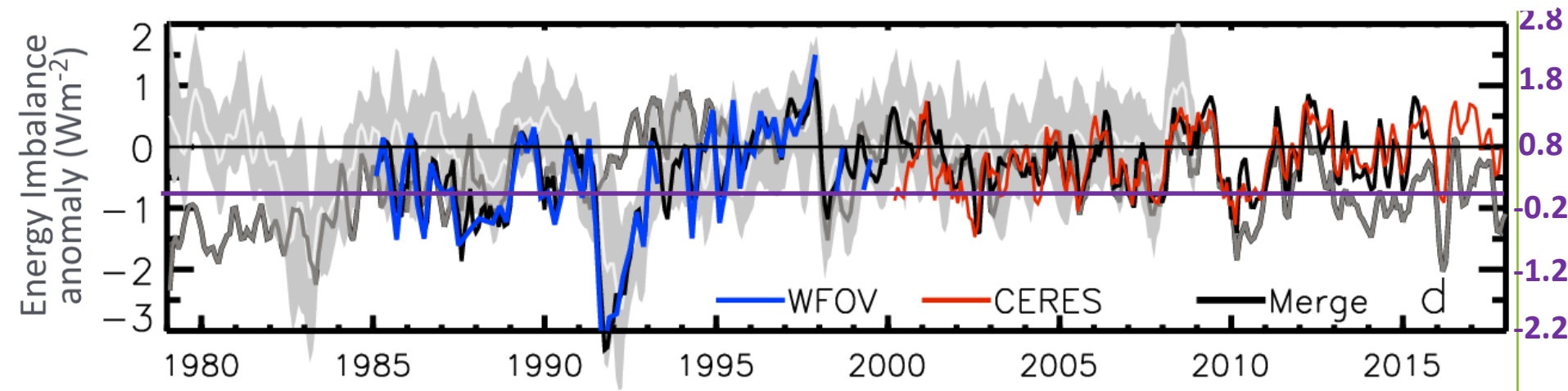


Longwave Top of the Atmosphere Flux



RECENT GLOBAL EEI VARIABILITY

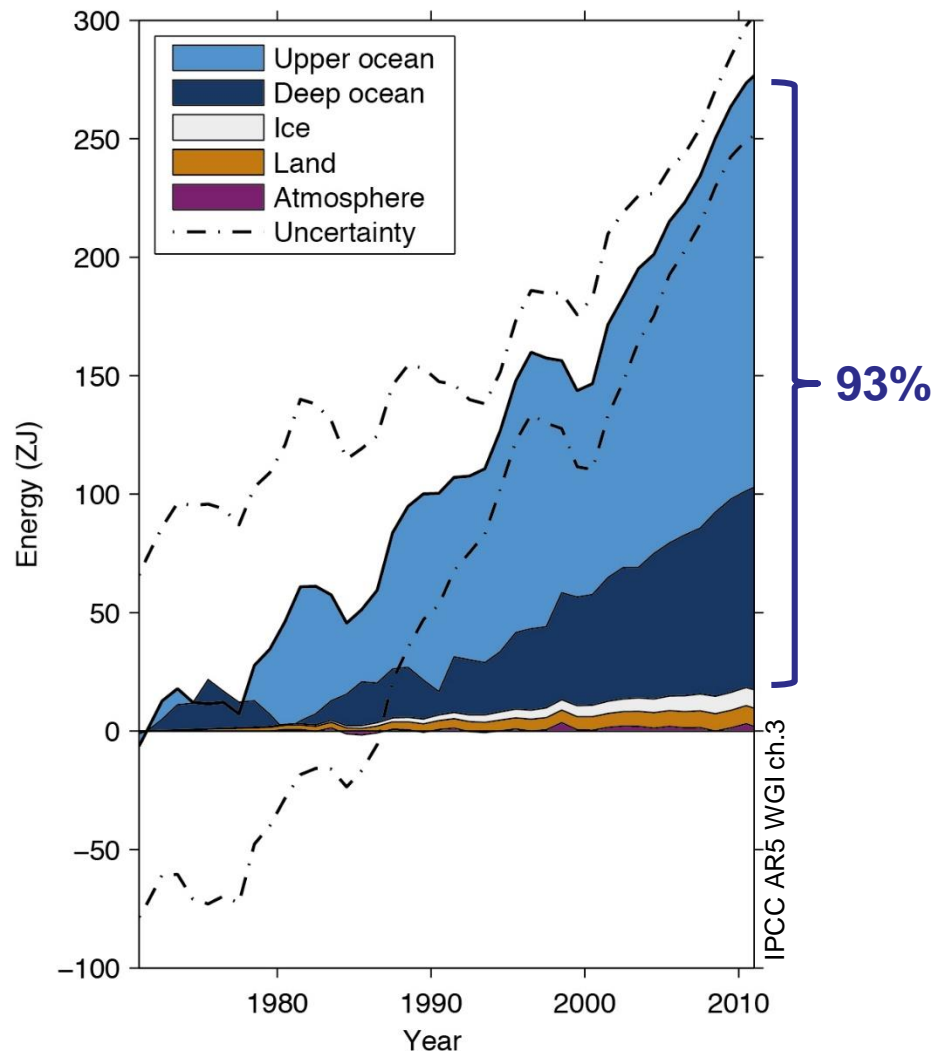
- Update from Allan et al.(2014) Surv. Geophys.; Allan et al. (2014) GRL
- EEI estimate from combining remote sensing data, atmospheric reanalyses and climate model simulations
- Model simulations used for assessing discontinuities in observations
- Mismatch reanalysis/ satellite in early 1990s (Pinatubo) and since 2010 (increase absorption of solar radiation)



Bold grey: ERAINT; thin light grey with envelope: AMIP5
Purple line: zero imbalance

Where does the excess heat go?

- Plot of energy accumulation in ZJ (1 ZJ = 10^{21} J) within distinct components of the Earth's climate system relative to 1971 and from 1971 to 2010 unless otherwise indicated.
- Ocean warming (heat content change) dominates, with the upper ocean (light blue, above 700 m) contributing more than the mid-depth and deep ocean (dark blue, below 700 m; including below 2000 m estimates starting from 1992).
- Ice melt (light grey; for glaciers and ice caps, Greenland and Antarctic ice sheet estimates starting from 1992, and Arctic sea ice estimate from 1979 to 2008); continental (land) warming (orange); and atmospheric warming (purple; estimate starting from 1979) make smaller contributions.
- Uncertainty in the ocean estimate also dominates the total uncertainty (dot-dashed lines about the error from all five components at 90% confidence intervals).



Four ways to estimate the global ocean heat content (OHC)

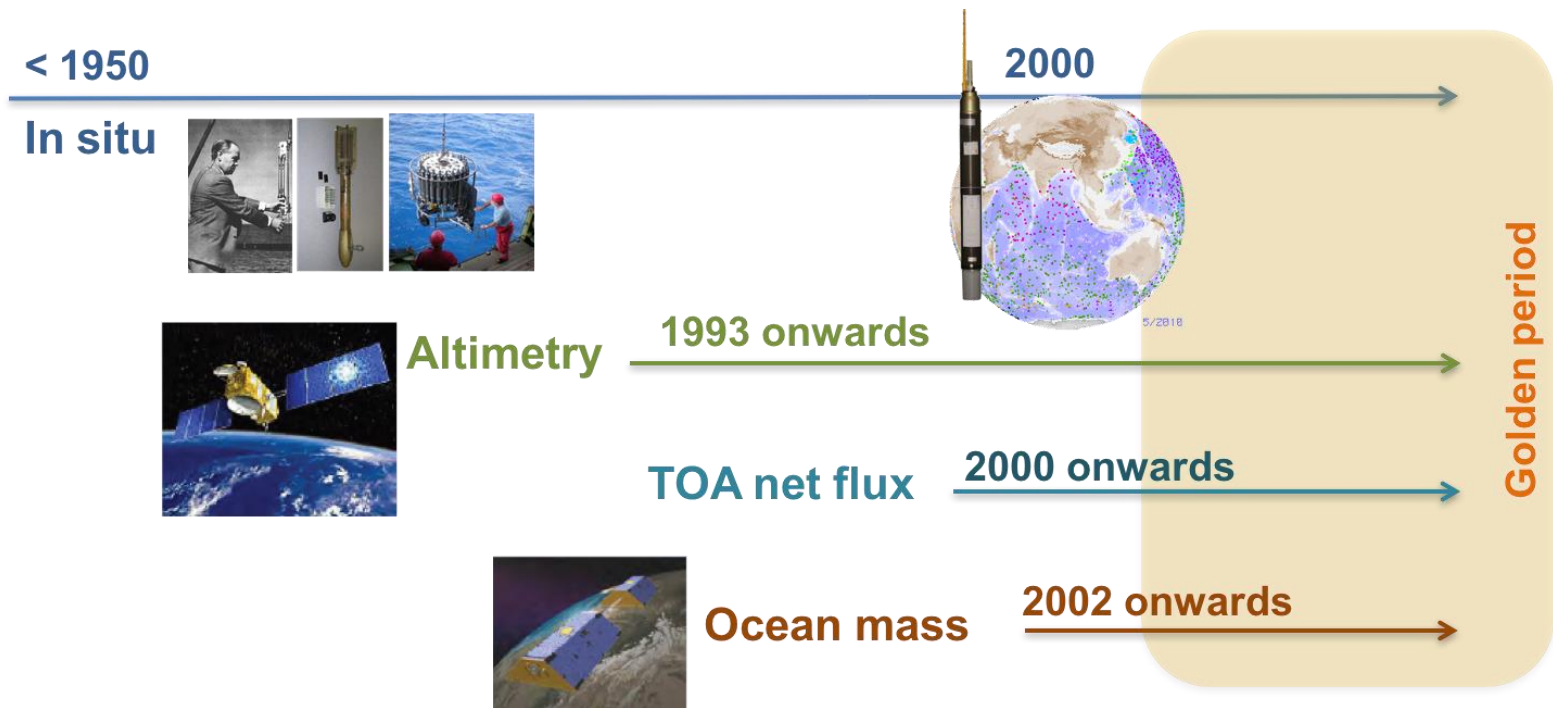
$$OHC = \int \rho C_p \Theta dV$$

ρ : seawater density
 C_p : specific heat capacity
 Θ : conservative temperature

Usually discuss **anomalies** of ocean heat content and conservative temperature: **15 ZJ or 0.015 K/yr**

- 1) Direct measurement of in-situ temperature
- 2) Remote sensing of the net ocean surface heat fluxes
- 3) Remote sensing of the thermal expansion of the ocean
- 4) Estimate from reanalyses assimilating both in-situ and remote observations

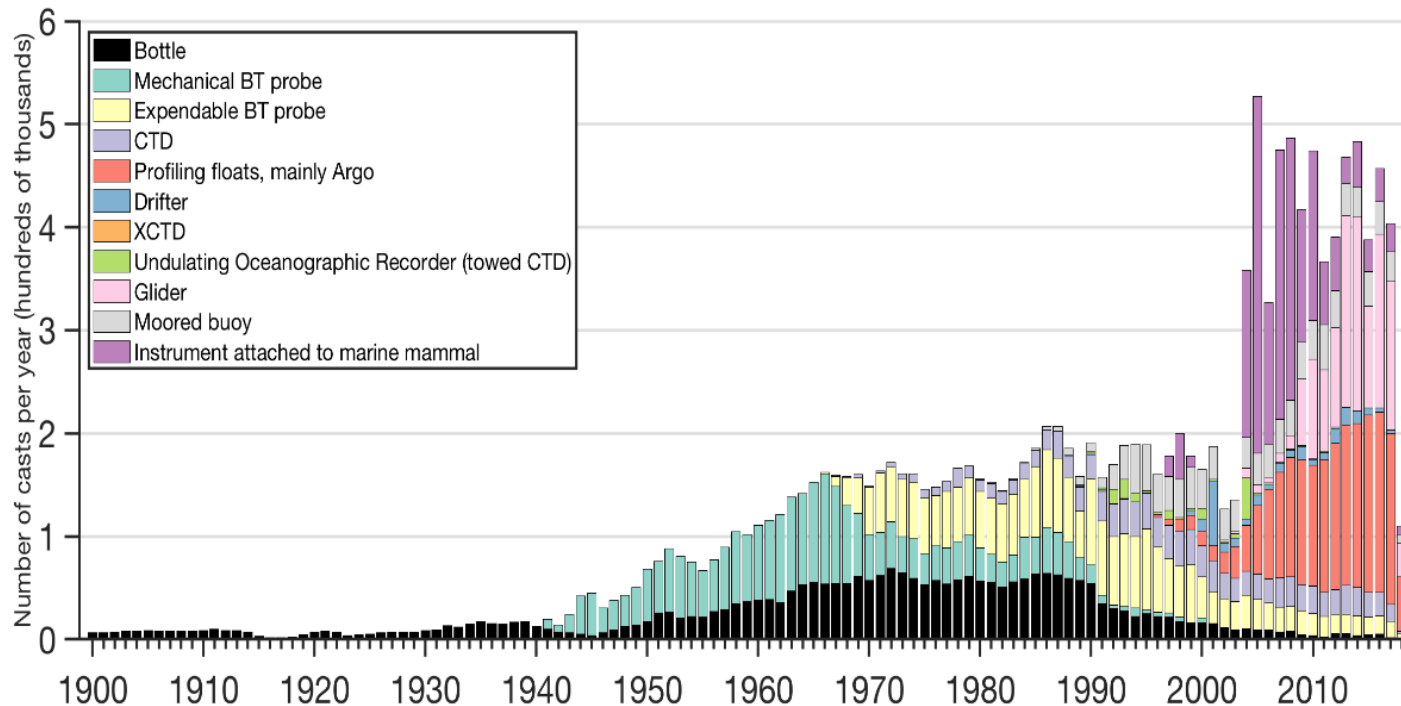
Observing the world ocean's heat content



Meyssignac et al., 2019, under review

$$\Delta SL_{\text{thermsteric}} = \Delta SL_{\text{total}} - \Delta SL_{\text{mass}}$$

In-situ observations

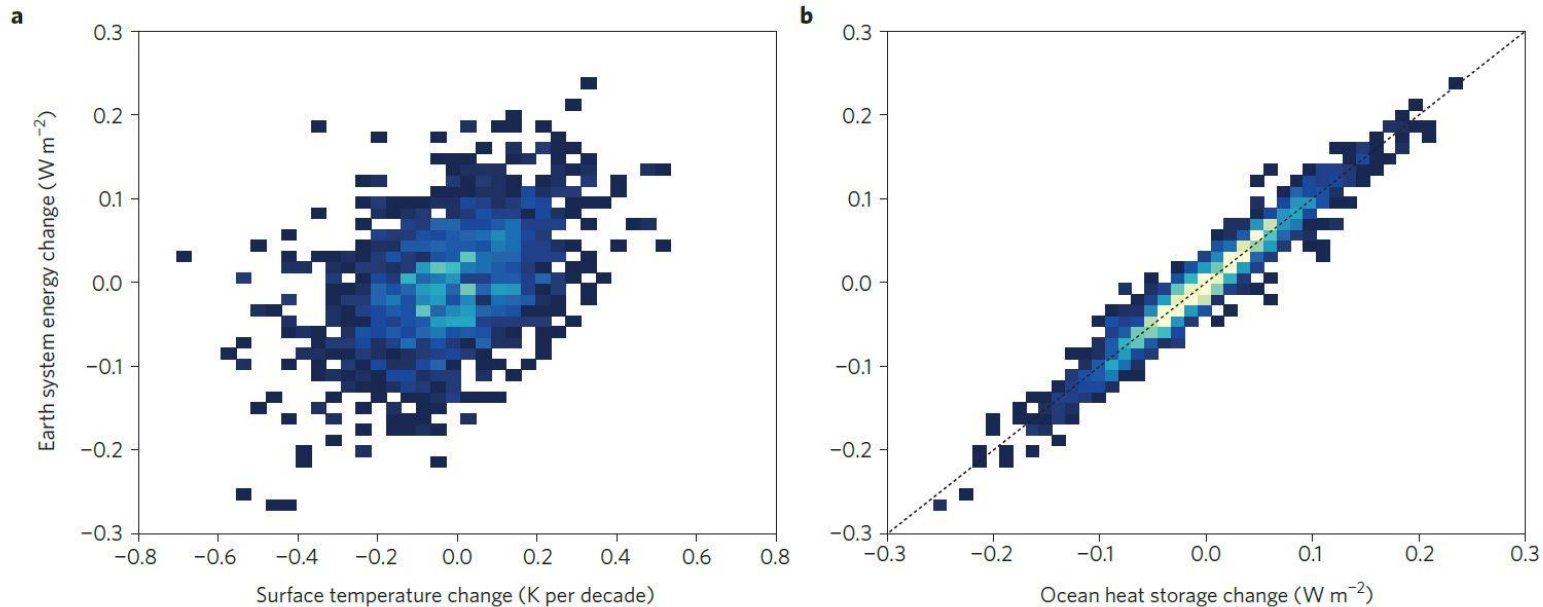


Meyssignac et al., 2019, under review

Number of subsurface ocean temperature profiles per year by instrument type 1900–2017. BT=Bathythermograph, CTD=Conductivity-Temperature-Depth, XCTD=Expendable CTD

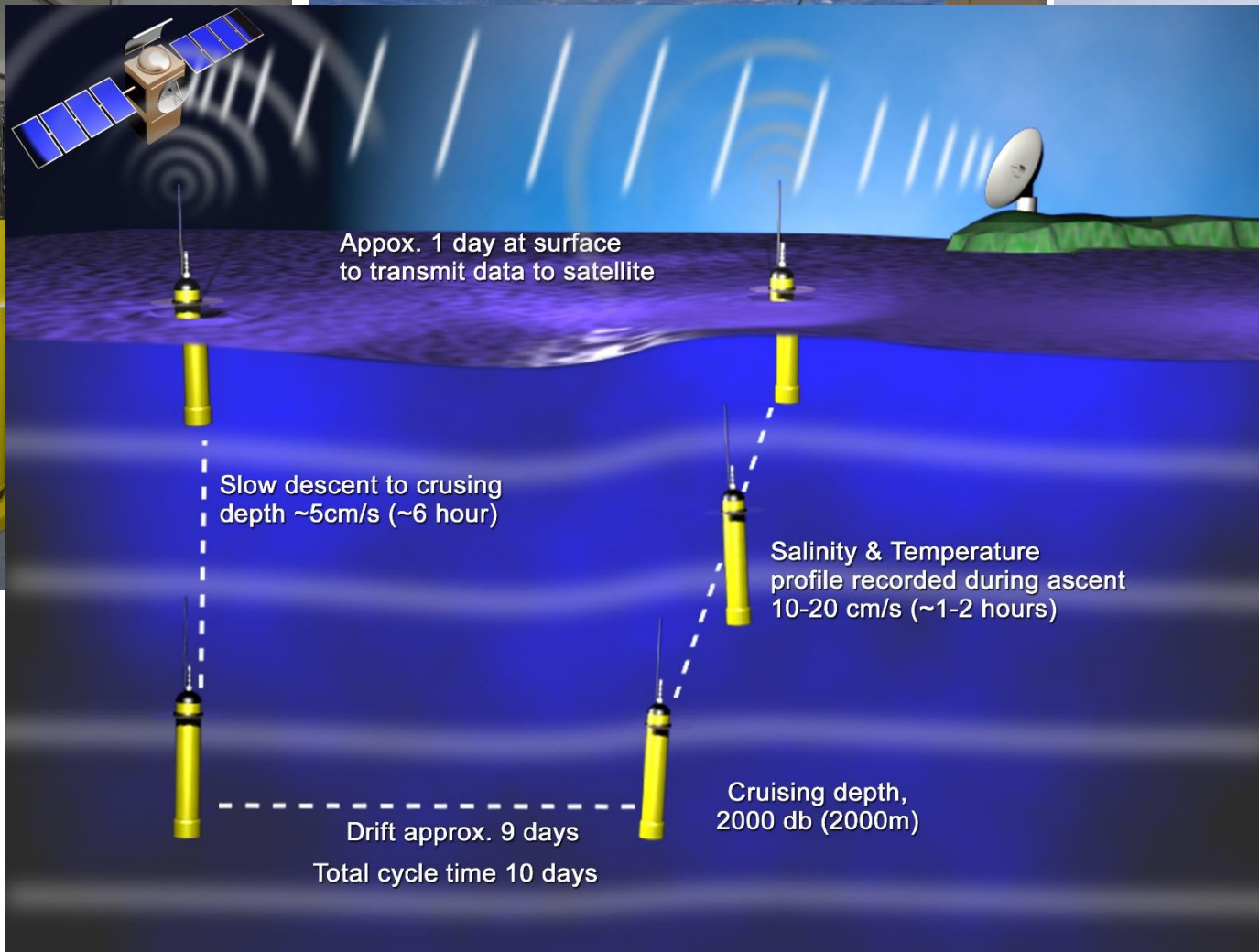
- Many more measurements from the ocean's surface ...

... but (full-) depth coverage is much more useful



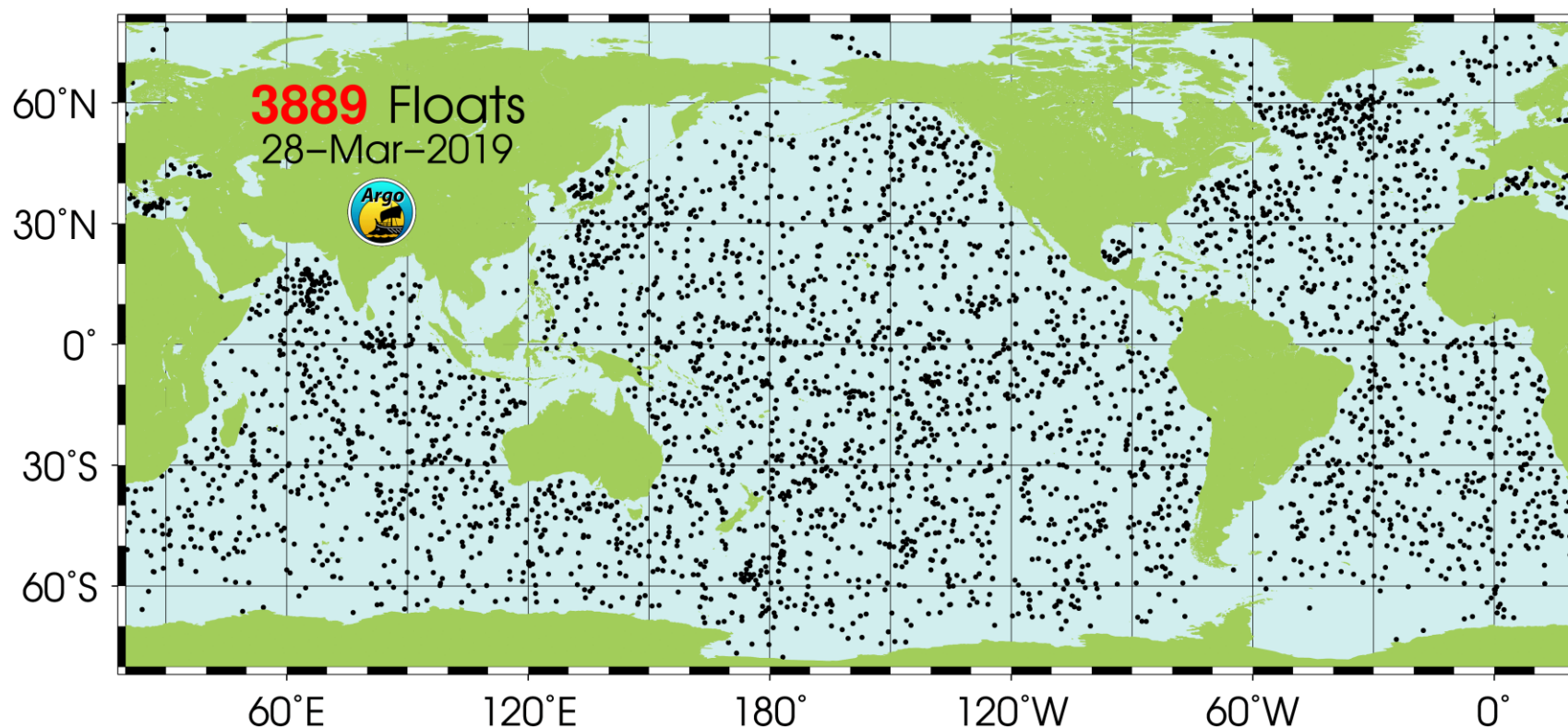
- Ocean heat content more indicative of Earth's energy imbalance trend than sea surface temperature

ARGO autonomous floats



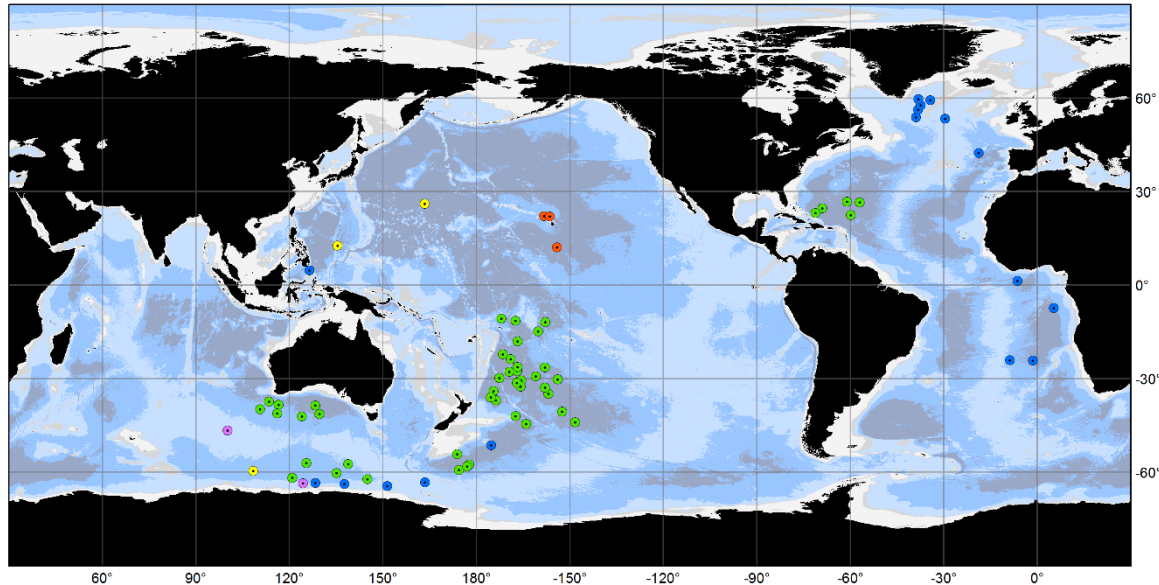
ARGO coverage

Positions of the floats having delivered data in the preceding 30 days



- ~ 3,800 free-drifting profiling floats that measure the temperature and salinity of the upper 2000 m of the ocean

Deep ARGO



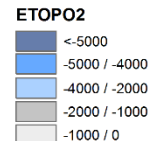
Argo

Deep Float Models

February 2019

Latest location of operational floats (data distributed within the last 30 days),

- SOLO_D_MRV (3)
- NINJA_D (2)
- APEX_D (3)
- SOLO_D (48)
- ARVOR_D (17)



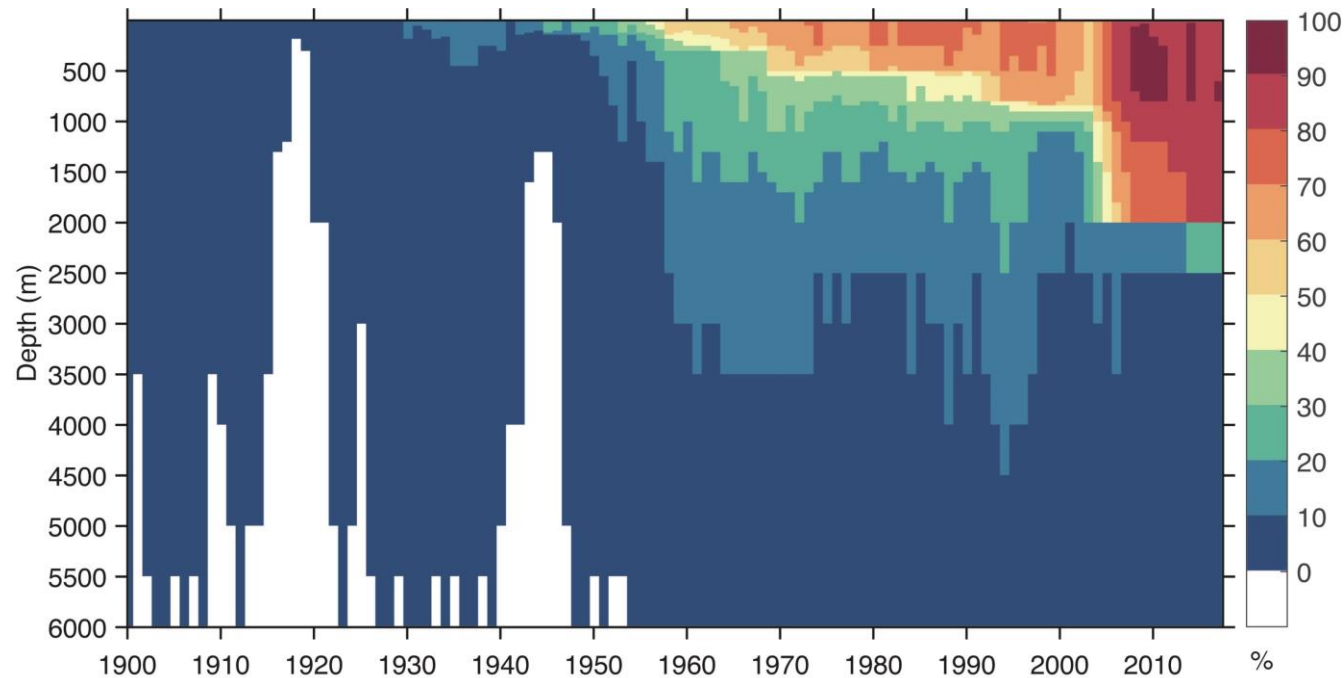
Generated by www.jcommops.org, 08/03/2019



- Extension of Argo network to 4000 m/ 6000 m deep sampling is under way (currently ~75 test floats)

Sources of uncertainty

- Instrument bias: MBT/ XBT drop rate; Argo float pressure sensors
- Data coverage: infill methods/ mapping

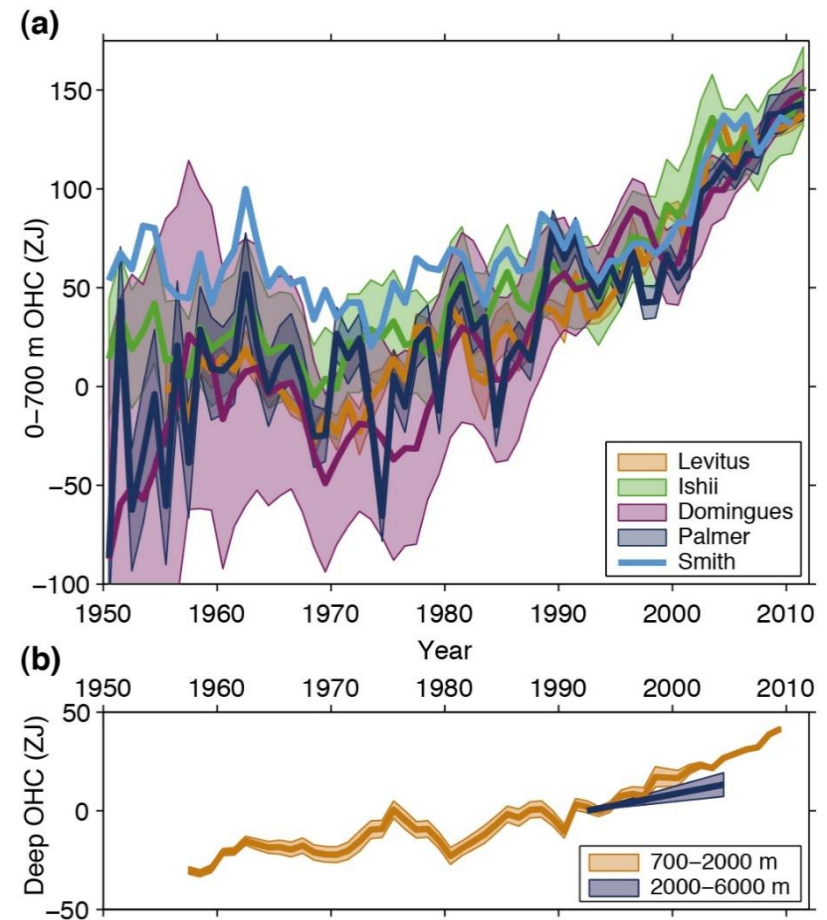


Meyssignac et al., 2019, under review

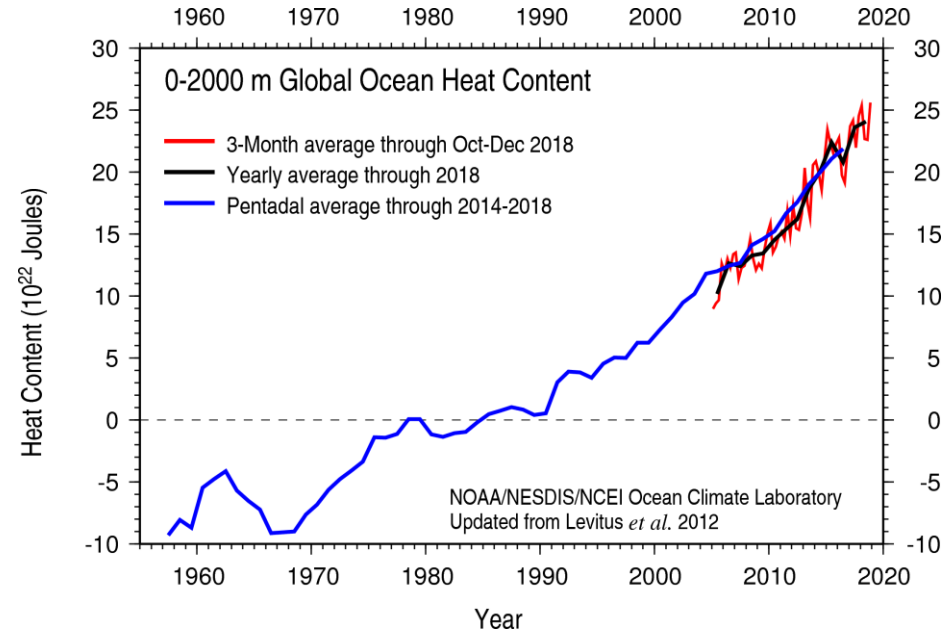
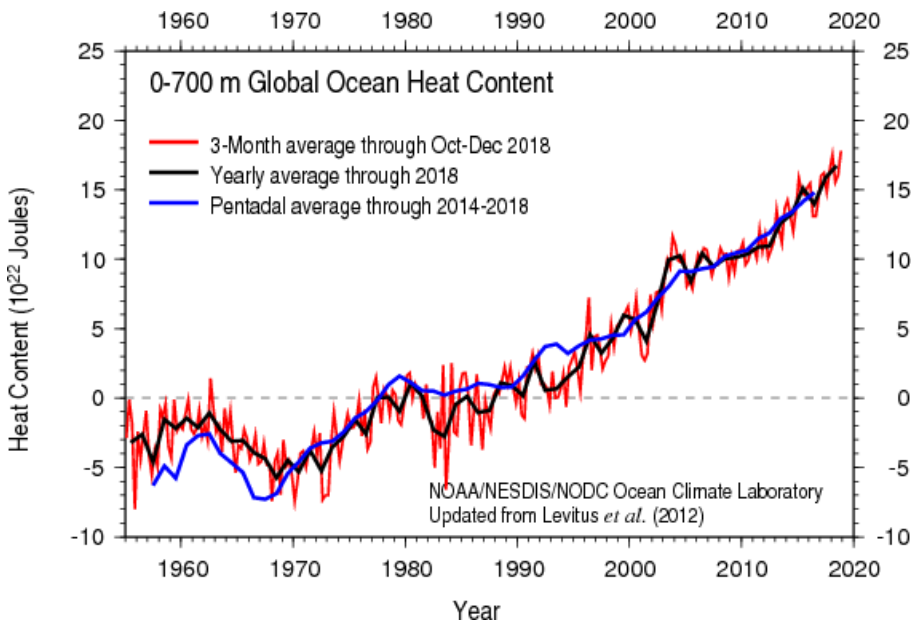
Percentage of data coverage for 3x3 boxes over the global ocean area from 5m to 6000m

Ocean heat uptake: observed

- IPCC AR5, Figure 3.2: | (a) Observation-based estimates of annual global mean upper (0 to 700 m) ocean heat content in ZJ (1 ZJ = 1021 Joules) updated from (see legend): Levitus et al. (2012), Ishii and Kimoto (2009), Domingues et al. (2008), Palmer et al. (2007) and Smith and Murphy (2007). Uncertainties are shaded and plotted as published (at the one standard error level, except one standard deviation for Levitus, with no uncertainties provided for Smith). Estimates are shifted to align for 2006–2010, 5 years that are well measured by Argo, and then plotted relative to the resulting mean of all curves for 1971, the starting year for trend calculations. (b) Observation-based estimates of annual 5-year running mean global mean mid-depth (700 to 2000 m) ocean heat content in ZJ (Levitus et al., 2012) and the deep (2000 to 6000 m) global ocean heat content trend from 1992 to 2005 (Purkey and Johnson, 2010), both with one standard error uncertainties shaded (see legend).

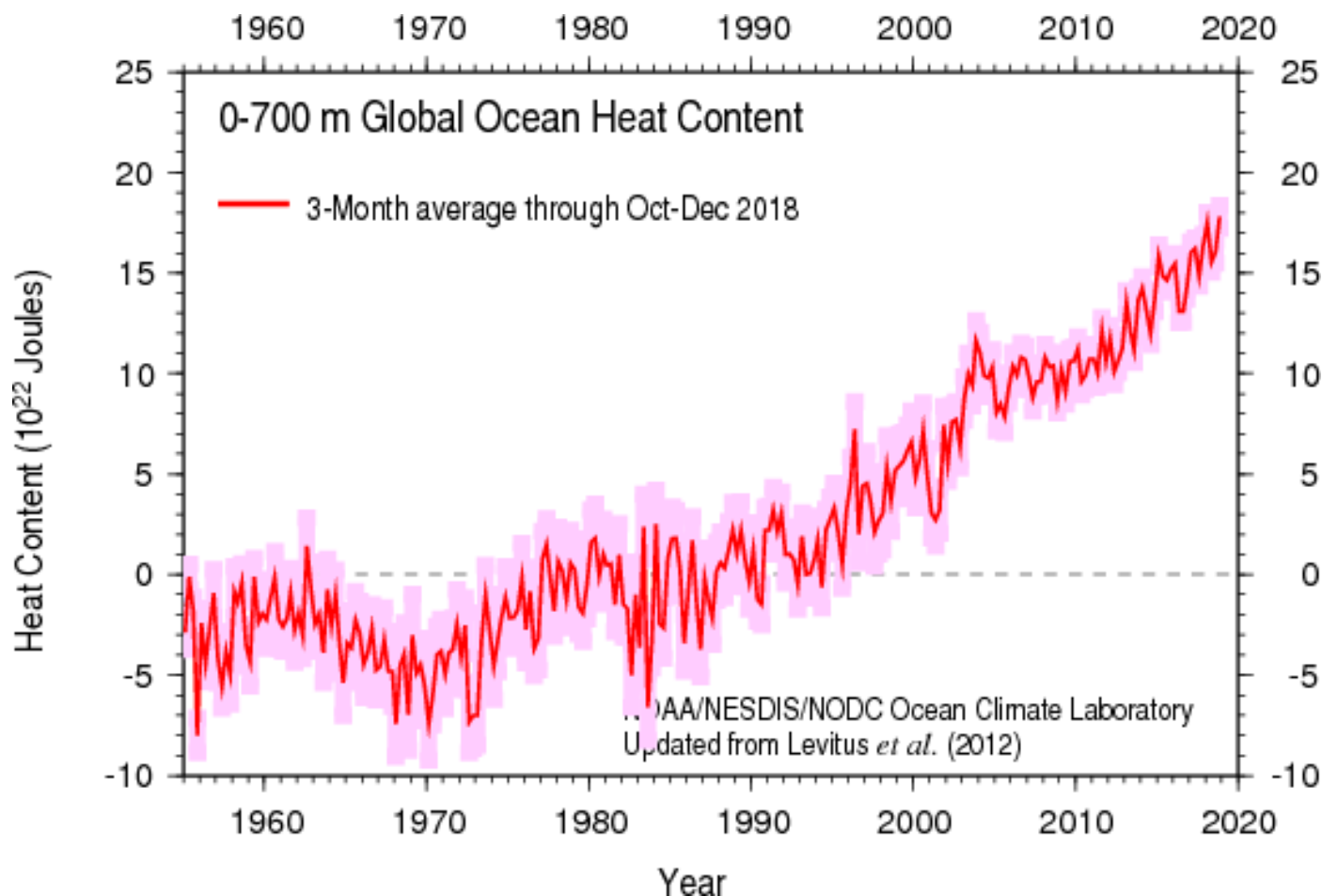


Ocean heat content observations: NOAA/NCEI



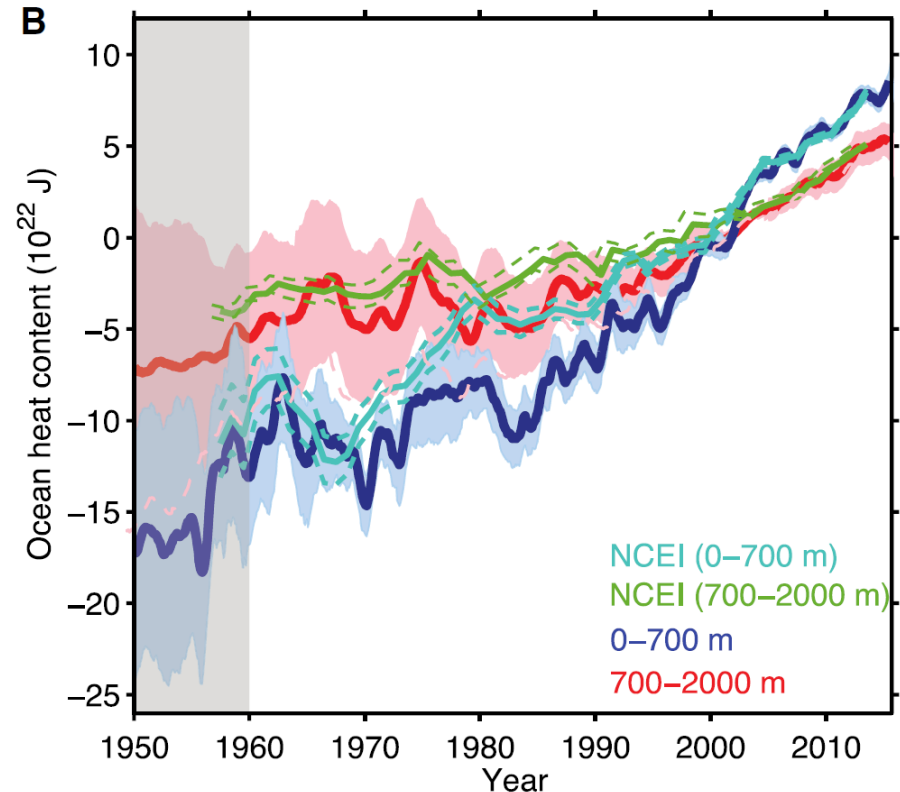
- ① Extension of Levitus *et al.* (2012)
- ① 2018 warmest year since 1955

Ocean heat content observations: NOAA/NCEI with uncertainties



OHC: Minimize sampling error

- ⦿ Cheng et al. (2017), Sci. Adv. 3
- ⦿ Bin/ collect data for spatial regions and time windows (standard technique)
- ⦿ Attempt at removing aliased signal from mesoscale features
- ⦿ Subsample test: subsets of data during the data rich Argo era are co-located with locations of earlier ocean observations, to quantify sampling error
- ⦿ Inferred EEI is larger than in previous assessments



Some independent net OHC and EEI estimates

table S2. Net OHC and EEI changes obtained in the current study compared with some independent estimates. The independent estimates come from several published studies including *Cheng et al. (63)*, *Allan et al. (65)*, and *IPCC-AR5 (1)*.

	Source	Full-depth OHC ($\times 10^{22}$ J)	EEI ($\times 10^{22}$ J)	
1960–2015	This study	33.5 \pm 7.0	36.0 \pm 7.5	
1970–2005	This study	26.5 \pm 4.8		
1970–2005	Adjusted observational OHCs and ORAS4 (63)	28.3 \pm 1.8		
1970–2005	CMIP5 (63)	26.6 \pm 4.4		
1993–2008	This study		18.7 \pm 1.1	
1993–2008	TOA (65)		16.7 \pm 17.2 (0.65 \pm 0.67 W/m ²)	
1971–2010	This study	28.8 \pm 4.4	31.0 \pm 4.7	
1971–2010	IPCC-AR5 (1)	25.5 \pm 6.1	27.4 \pm 7.8	

Cheng et al., Sci. Adv. 2017, 3

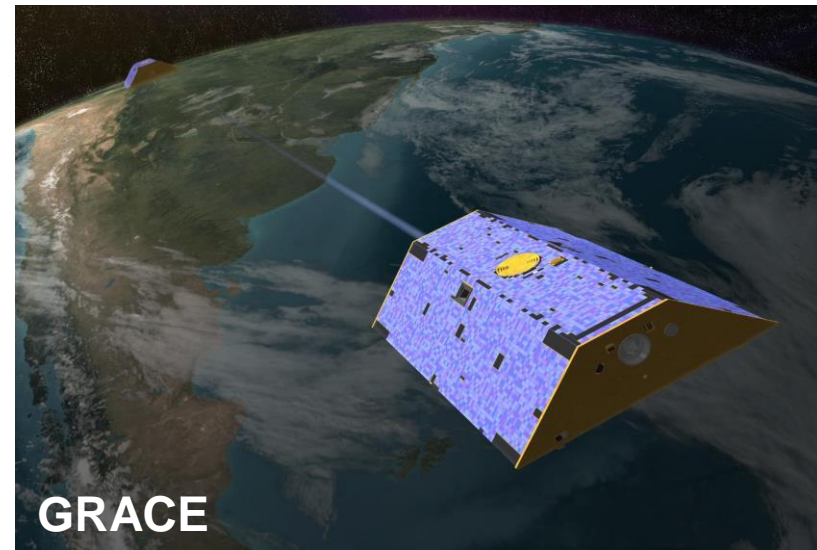
- ⦿ Cheng et al., 2016, Ocean Sci. 12
- ⦿ Allan et al., 2014, GRL 41

Remote sensing of thermosteric sea level rise

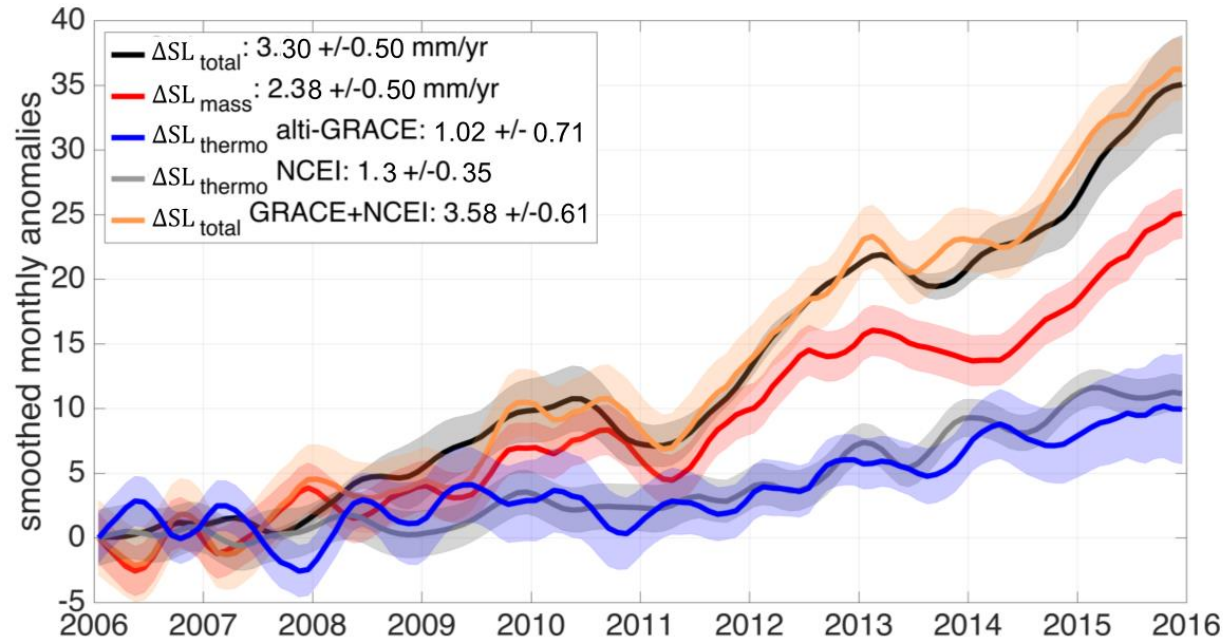
$$\Delta SL_{total} = \Delta SL_{mass} + \Delta SL_{thermo}$$

$$\Delta OHC_{altim-GRACE} = \frac{\Delta SL_{thermo}}{\epsilon}$$

- Altimeters measure sea level
 - No data coverage close to poles; remote sensing of SL under sea ice cover difficult
- GRACE: Gravity Recovery And Climate Experiment
 - Measures mass changes of ocean, ice, land



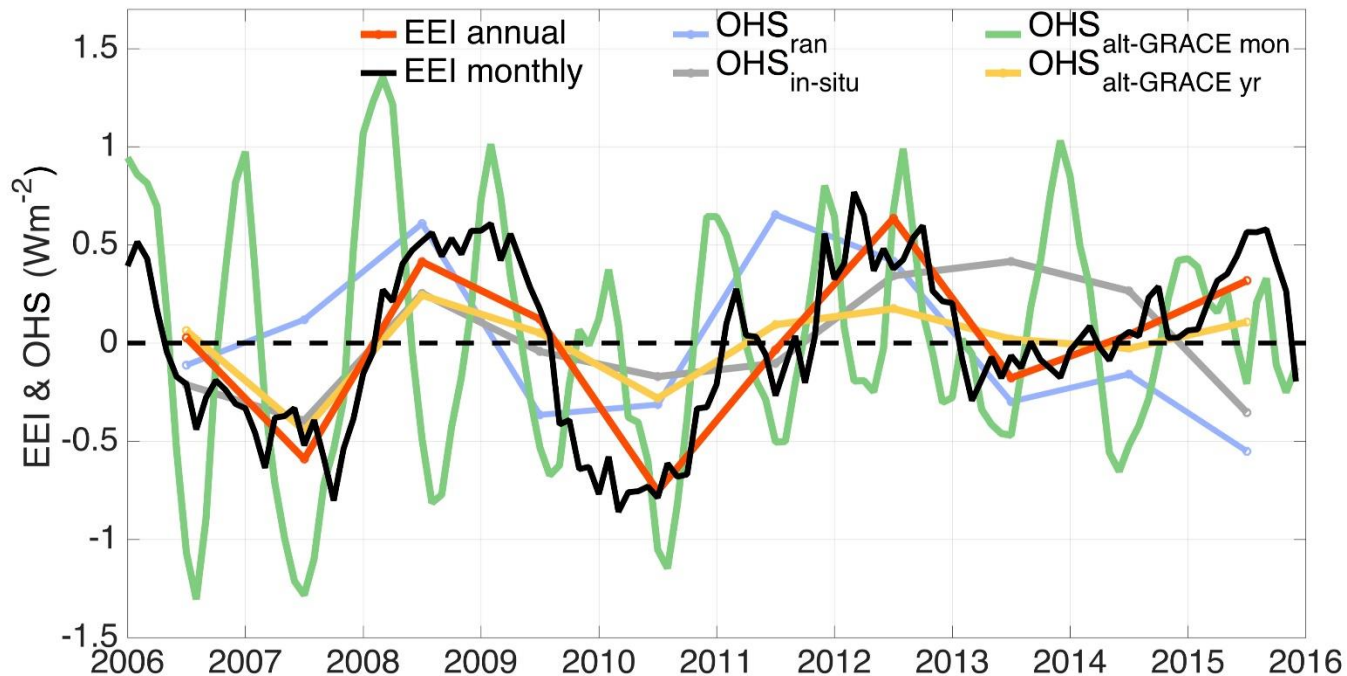
Remote sensing of thermosteric sea level rise



Meyssignac et al., 2019, under review

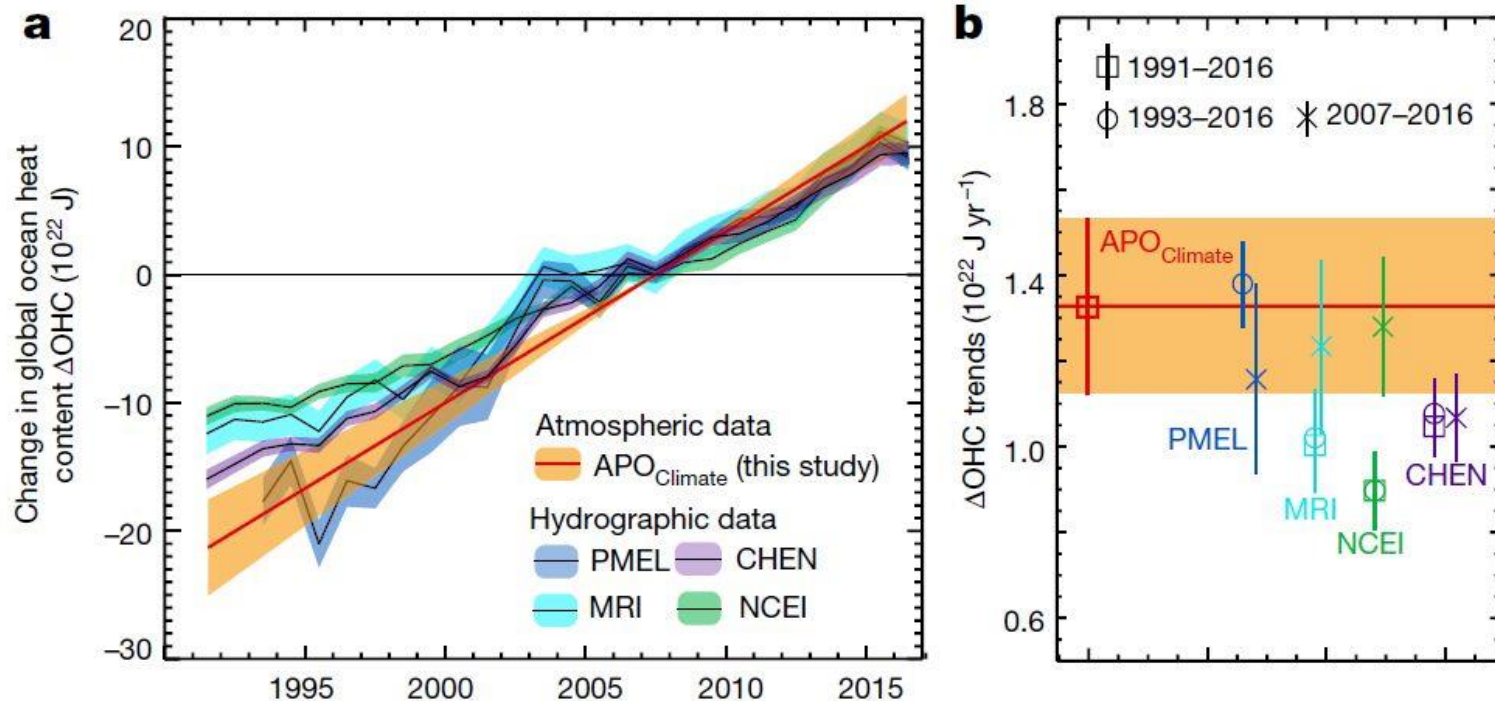
- Global mean anomalies of total sea level in mm (monthly anomalies, 5-months running means) derived from six altimetry data sets (ΔSL_{total} , black), ocean mass change from four GRACE products (ΔSL_{mass} , red), thermosteric sea level change as the residual of $\Delta SL_{thermo} = \Delta SL_{total} - \Delta SL_{mass}$ (blue), ΔSL_{thermo} from NOAA NCEI (gray) based on interpolated seasonal anomalies, and ΔSL_{total} as the sum of ΔSL_{thermo} from NCEI and ΔSL_{mass} (orange). The shadings indicate the measurement uncertainty (5-95% CL)

EEl interannual variability from different sources



EEI (CERES EBAF) and OHS (dOHC/dt) timeseries from ocean reanalysis (OHS_{ran}), *in situ* estimation (OHS *in situ*), and alti-GRACE (OHS_{alti-GRACE}). We show annual timeseries for all parameters (with long-term mean removed) and deseasonalized monthly anomalies for OHS_{alti-GRACE} and EEI that have been smoothed applying a 5-months running average filter.

OHC: an independent estimate



Resplandy et al. (2018), Nature

- Change in global ocean heat content (ΔOHC). a, ΔOHC derived from hydrographic and atmospheric observations (normalized to zero in 2007, $\pm 1\sigma$ uncertainty). b, Linear least-squares trends for 1991–2016, 1993–2016 and 2007–2016 ($\pm 1\sigma$ uncertainty). Hydrography-based ΔOHC estimates combine warming rates at ocean depths of 0 to 2,000 m (from Cheng and co-authors (CHEN)¹², Pacific Marine Environmental Laboratory (PMEL)¹⁰, Meteorological Research Institute (MRI)⁹ and National Centers for Environmental Information (NCEI)³¹ estimates) with the revised deep ocean warming (at depths of more than 2,000 m) of ref. 11 (Extended Data Tables 1 and 2). The atmospheric-based estimate (this study), which uses **observed atmospheric potential oxygen trends ($\Delta\text{APO}_{\text{Climate}}$) and model-based $\Delta\text{APO}_{\text{Climate}}$ -to- ΔOHC ratios**, does not resolve interannual variations.
- The error estimates are substantially too small

Uncertainties in the OHU trend

Full-depth OHU trend estimates, 2006-2015 (as reviewed by Meyssignac et al., 2019)

- ⦿ In-situ: $0.65 \pm 0.11 \text{ W m}^{-2}$ (Johnson et al., 2018)
- ⦿ alti-GRACE: $0.53 \pm 0.38 \text{ W m}^{-2}$
- ⦿ *Net ocean surface heat flux: $(10 \dots 15) \pm 15 \text{ W m}^{-2}$*
- ⦿ Reanalyses: $0.74 \pm 0.14 \text{ W m}^{-2}$

What needs to be done



- ⦿ Sustain observations: ocean temperature (Argo floats) and sea level (remote sensing, tide gauges)
- ⦿ Increase spatial coverage:
 - Deep Argo (below 2,000 m)
 - Regions not covered by Argo: sea-ice covered regions, shelf seas, marginal seas
 - Satellite altimetry of polar regions
- ⦿ Uncertainties: quantify and reduce
 - Independent observation of in-situ temperature to cross-validate Argo
 - Improve confidence in ocean mass estimates from GRACE: independent verification through mass estimate from freshwater budget/salinity record